JTTEE5 17:878–886
DOI: 10.1007/s11666-008-9285-y
1059-9630/$19.00 © ASM International

Plasma Sprayed Coatings of High-Purity Ceramics for Semiconductor and Flat-Panel-Display Production Equipment

Junya Kitamura, Hiroyuki Ibe, Fumi Yuasa, and Hiroaki Mizuno

(Submitted May 15, 2008; in revised form August 12, 2008)

High-purity oxide ceramic powders of alumina (Al_2O_3) and yttria (Y_2O_3) have been developed to apply to semiconductor and flat-panel-display (FPD) production equipment. The ceramic coatings on the inside chamber wall of the equipment are required to have high erosion resistance against CFx plasma in dry etching process for microfabrications of the devices. It is found that the yttria coating formed from agglomerated-and-sintered powder consisting of large primary particles has smoother eroded surface with high erosion resistance. Considering the particle deposition on the devices, this coating will be effective in decreasing generation of large-sized particles, which easily deposit on the devices. Electric insulating properties of the coatings are also investigated to apply to electrostatic chuck. Electric breakdown voltage of yttria coatings is comparable to that of alumina coatings. Smaller powder is effective for improving the electric properties, and the influence of coating purity is lower than that of the powder size.

Keywords alumina, APS coatings, erosion and abrasion resistance, high-purity ceramics, semiconductor applications, yttria

1. Introduction

The size of semiconductor and flat-panel-display (FPD) production equipment for dry etching, sputtering, and ashing has been increasing due to the increasing size of Si wafer (from 200 to 300 mm in diameter) and of the FPD, where plasma treatment is effectively used for micro fabrication especially in dry etching. Applied power for generating plasma is also increasing to fabricate the Si and LCD devices uniformly onto the large-scaled substrates. This trend strongly promotes application of plasma sprayed coatings by high-purity ceramics for anti-plasma erosion at inside chamber wall and for high electric strength (high breakdown voltage) of electrostatic chuck (ESC) to replace from conventional techniques, such as anodized aluminum (alumite film) and sintered bulk ceramics (Ref 1, 2). For example, inner diameter of the chamber wall is increasing from 400 to 500-600 mm in the Si device production equipment due to the enlargement of the wafer size.

Using the alumite film as a shield or an ESC to protect the chamber parts has been difficult because the halogen-containing plasma with high power erodes the film at a high rate. This intense erosion generates a large amount of particles and results in frequent maintenance of the production equipment and decrease of yield ratio of the devices. Sintered bulk ceramics are also difficult to be used as the shielding parts by the enlargement of the equipment because production of large-scaled ceramics is technically difficult and its cost tends to become high.

Plasma sprayed ceramics coatings have technical and commercial advantages to overcome these problems, such as no limitation of the equipment size, relatively higher anti-plasma erosion resistance, higher breakdown voltage, and relatively low cost to make thick coating of about a few hundred micrometers. As ceramic materials for plasma spraying, aluminum oxide (alumina, Al_2O_3) and yttrium oxide (yttria, Y_2O_3) have been utilized presently due to their high durability against the halogen-containing plasma (Ref 2, 3). In particular, spraying technique seems to be better for yttria because of its high brittleness and high cost compared with alumina.

Our recent systematic investigations have revealed that plasma sprayed Y_2O_3 coatings have higher plasma erosion resistance than Al_2O_3 coatings as well as sintered-bulk Al_2O_3 against CF_4/O_2 at wide-ranged plasma power conditions including the actual conditions in semiconductor fabrication processes (Ref 4, 5). However, the resistance is still inferior to sintered-bulk Y_2O_3 showing that further

This article is an invited paper selected from presentations at the 2008 International Thermal Spray Conference and has been expanded from the original presentation. It is simultaneously published in *Thermal Spray Crossing Borders, Proceedings of the 2008 International Thermal Spray Conference*, Maastricht, The Netherlands, June 2-4, 2008, Basil R. Marple, Margaret M. Hyland, Yuk-Chiu Lau, Chang-Jiu Li, Rogerio S. Lima, and Ghislain Montavon, Ed., ASM International, Materials Park, OH, 2008.

Junya Kitamura, Hiroyuki Ibe, Fumi Yuasa, and **Hiroaki Mizuno**, Thermal Spray Materials Department, Fujimi Incorporated, Kakamigahara, Gifu Pref. 509-0103, Japan. Contact e-mail: kitamuraj@fujimiinc.co.jp.

improvement is required for plasma spray coating. Recently, $Ar/CF_4/O_2$ plasma is increasingly being used in the actual device fabrication at plasma etching process (Ref 3). Ar addition enhances physical etching effect as well as reduces chemical etching effect, which results in increasing etching rate and high capability of making deep and narrow structures that are required to fabricate highly integrated circuits for next generation.

In this paper, the structural properties of Al_2O_3 and Y_2O_3 coatings have been investigated to understand the mechanism of the plasma erosion resistance under $Ar/CF_4/O_2$ and CF_4/O_2 plasma conditions using reactive ion etching (RIE) system, which is generally used for dry etching process. The influence of the plasma gas composition and mechanism of the erosion are also discussed with the help of the microstructural analysis using scanning electron microscopy (SEM). Dielectric breakdown properties, key properties for ESC, have also been measured to investigate the effect of coating structure.

2. Experimental Procedure

2.1 Spray Powders

Al_2O_3 powders used in this study are summarized in Table 1. Coarse (A1) and fine (A2) powders with purity of more than 99.9% were prepared by fused-and-crushed process. A3 powder produced by Sumitomo Chemical Co., Ltd. (Japan), whose size was comparable to A2, was also selected. This powder was prepared by vaporization method and its purity was more than 99.99%. Fused-and-crushed A4 (99.6%) was a much finer powder with an average size of 3.1 μm, which was used for fine powder high velocity oxy-fuel (HVOF) spraying system (Ref 6).

Table 2 summarizes agglomerated-and-sintered Y_2O_3 powders used in this study, in which the primary-particle diameter was changed ranging from 0.6 to 5.3 μm (Y1-Y3). The powder size distribution and purity were

Table 1 Spray powders and bulk of Al_2O_3

Name	Purity, %	Manufacturing methods	Average diameter, μm	Powder size distribution, μm
A1	99.9	Fused & crushed	29.6	−45 + 15
A2	99.9		25.8	−38 + 8
A3	99.99	Vaporization	24.9	−38 + 10
A4	99.6	Fused & crushed	3.1	−5 + 1
AB	99.9	Sintered bulk (as a reference)		

Table 2 Spray powders and bulk of Y_2O_3

Name	Purity, %	Manufacturing methods	Average diameter, μm	Primary-particle diameter, μm
Y1	99.9	Agglomerated	39	0.6
Y2		& sintered	36.3	2.9
Y3			42.8	5.3
YB	99	Sintered bulk (as a reference)		

−63 + 10 μm and 99.9%, respectively. All Al_2O_3 and Y_2O_3 powders except for A3 were prepared by Fujimi Incorporated (Japan). SEM images of the spray powders are shown in Fig. 1. Both sintered-bulk Al_2O_3 (AB) and Y_2O_3 (YB), whose sizes were 15 × 15 × 2.0^t mm, were used for the plasma erosion test, as a reference. Sintered-bulk ceramics were prepared by Tsukuba Ceramic Works (Japan).

2.2 Preparation of the Specimens

Plasma spray and HVOF conditions are summarized in Table 3. Atmospheric plasma spraying by SG-100 (Praxair, USA) was conducted to prepare the coatings except for A4 powder. HVOF spraying by theta-gun (WHITCO, Japan) was used to prepare Al_2O_3 coating by A4 powder, where acetylene injection ports were added at the downstream of powder ports to generate higher temperature flame (Ref 6). Substrates of aluminum alloy (A6061) were sand-blasted by alumina grit of F40 prior to plasma spraying. The size of the substrates was 15 × 15 × 2.0^t mm for plasma erosion test and 50 × 70 × 5.0^t mm for dielectric breakdown test. The surfaces of sprayed coatings and sintered-bulk ceramics were mirror-polished using colloidal silica with an average diameter of 0.1 μm to study both the durability against the processing plasma and the erosion mechanism in detail for plasma erosion tests.

2.3 Plasma Erosion Test

Conditions of the plasma erosion tests under low and high power are summarized in Table 4 and 5, respectively. Durability of the coatings against CF_4/O_2 plasma was compared under the low and medium conditions (80 and 175 W). Effect of argon (Ar) addition in the plasma was studied at high power (400 W).

Before introducing into the reactive ion etching (RIE) chambers, the surface of the mirror-polished specimens was partially masked by polyimide tape at both sides. The eroded area was about 5 × 15 mm. The erosion rate was estimated by measuring the step height between masked area and eroded area using stylus method (Surfcom2000SD, Tokyo Seimitsu Co. Ltd., Japan). The Possibility of generating large-sized particle was studied through microstructural analysis of the eroded surface by SEM and the stylus method.

2.4 Dielectric Breakdown Test

A schematic of the dielectric breakdown test is illustrated in Fig. 2. A cylindrical electrode with 25 mm in diameter was placed on the specimen, which was followed by applying AC voltage with a ramp rate of 500 V/s at ambient air. Electric strength was estimated by dividing breakdown voltage by coating thickness. It is expected that electrical weak spot limits the measured breakdown voltage by such a large area contact than point contact. Considering the lower uniformity of plasma spray coatings and large ESC size in actual applications, this contact configuration will be better to compare the electric strength of the specimen quantitatively.

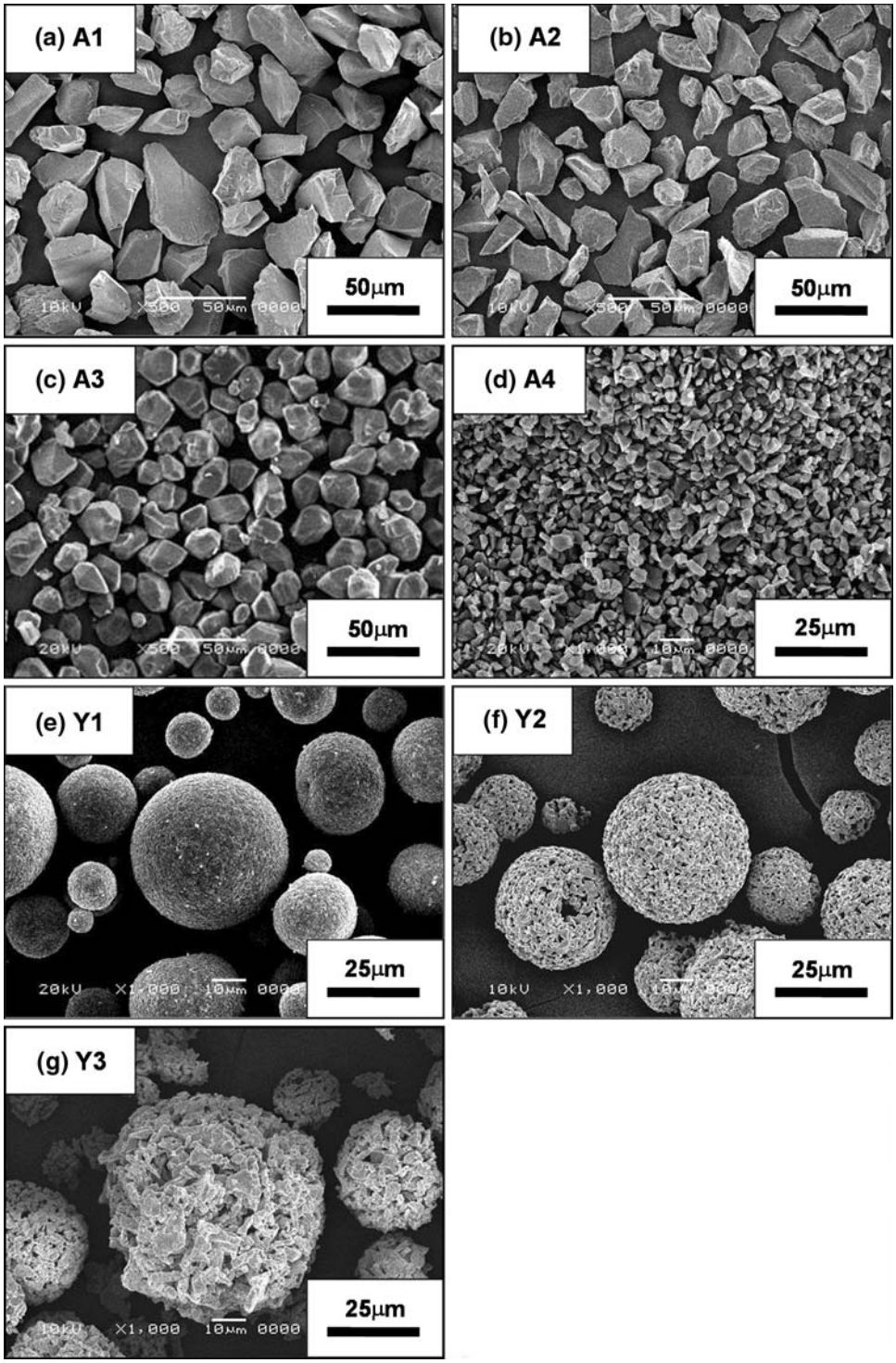

Fig. 1 SEM images of the (a-d) Al_2O_3 and (e-g) Y_2O_3 powders

3. Results and Discussion

3.1 Coating Structure of Al_2O_3 and Y_2O_3 Coatings

Figure 3 shows the cross-sectional SEM images of as-sprayed coatings. Lamellar structure is clearly seen in plasma sprayed Al_2O_3 coating of A1, which is consistent with previous report (Ref 7-12). A4 coating by fine powder HVOF system has quite a dense structure with high wear resistance (Suga abrasion test) and is mainly composed of α-phase for crystal structure (Ref 6). Density of all Y_2O_3 coatings seems to be higher in the SEM images and the porosity is observed by image analysis from

Table 3 Plasma and HVOF spray conditions

Equipments	Conditions	
Plasma SG-100 (Praxair)	Ar/He pressure, MPa	0.34/0.34
	Ar/He flow rate, L/min	39/7.9
	Arc current, A/voltage, V	900/36
	Spray distance, mm	120
HVOF θ-gun (Whitco)	Oxygen flow rate, L/min	893
	Kerosene flow rate, L/min	0.32
	Acetylene flow rate, L/min	43
	Spray distance, mm	150

Table 4 Plasma erosion test at low power

RIE equipment		RIE-200L (Samco Inc.)
CF_4 flow rate, L/min		0.054
O_2 flow rate, L/min		0.005
Chamber pressure, Pa		5
Plasma power, W		80
Exposure area, mm		200φ
Exposure time, min		480
Exposure cycle, min	Exposure	120
	Interval	60

Table 5 Plasma erosion test at medium and high power

Conditions	Medium	High	High
Gas compositions	CF_4/O_2	CF_4/O_2	$Ar/CF_4/O_2$
RIE equipment	RIE-200L	NLD-800 (ULVAC)	NLD-800
Ar flow rate, L/min	...	...	0.095
CF_4 flow rate, L/min	0.053	0.053	0.0095
O_2 flow rate, L/min	0.005	0.005	0.001
Chamber pressure, Pa	5	1	1
Plasma power, W	175	400	400
Exposure area, mm	200φ	100φ	100φ
Exposure time, min	480	60	60
Exposure cycle, min			
Exposure	120	0.5	0.5
Interval	60	3	3

optical micrographs. The A1 coating has higher porosity of 5% compared to the about 3% porosity of the Y1-Y3 coatings. It is suggested that Y_2O_3 melts easily than Al_2O_3 because of the porous shape of agglomerated-and-sintered powder during spraying process although melting point of Y_2O_3 (2410 °C) is higher than that of Al_2O_3 (2050 °C). The influence of primary Y_2O_3 particle size on the coating and crystal structure is unclear within this SEM observation because of the almost same porosity.

3.2 Plasma Erosion Test at Low Power (80 W)

Erosion rate of the spray coatings against CF_4/O_2 plasma at the low power (80 W) condition is shown in Fig. 4. Y_2O_3 coatings show lower erosion rate of about 1/5 times or less compared to the Al_2O_3 coatings suggesting that this large difference is mainly caused by material properties. Within the Al_2O_3 coatings, A2 and A3 coatings show high anti-erosion resistance suggesting that the effect of powder purity is small, ranging between 99.9 and 99.99%. Lower resistance of A1 coating might be derived from higher porosity because of using coarser powder.

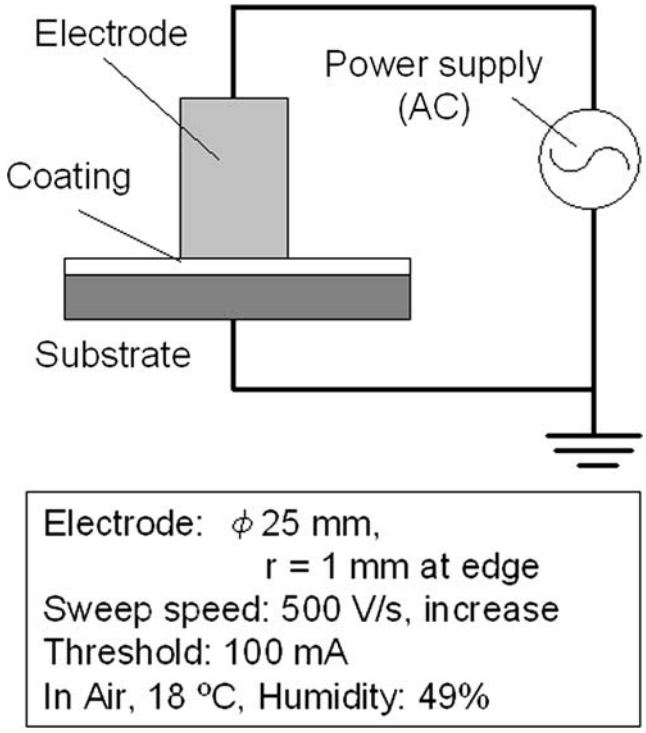

Fig. 2 A schematic of the dielectric breakdown test

On the other hand, other mechanisms should be considered for dense A4 coating. The effect of primary particle for Y_2O_3 coatings is low at the test condition.

3.3 Influence of Plasma Power (CF_4/O_2)

Figure 5 shows the erosion rates of the plasma sprayed coatings and the sintered-bulk by CF_4/O_2 plasma at both medium (175 W) and high (400 W) power conditions. At medium power, the order of durability is Y_2O_3 bulk (YB) > Y_2O_3 coatings (Y1-Y3) > Al_2O_3 bulk (AB) > Al_2O_3 coating (A2), showing the superiority of Y_2O_3 and sintered-bulk. The same tendency is seen at high power, showing that the order of the durability is independent of the plasma power within the conditions studied.

The Y_2O_3 coatings (Y1-Y3) have slightly better durability than the Al_2O_3 bulk (AB) at low plasma power. Y3, best within the Y_2O_3 coating, has higher durability of 2 times that of Al_2O_3 bulk. When increasing the plasma power, the durability of the Y_2O_3 coatings compared to the Al_2O_3 bulk becomes much better—about 3-4 times. The same tendency is obtained between Y_2O_3 coatings and Y_2O_3 bulk (YB). Although Y_2O_3 bulk has higher durability at both the powers, the durability difference becomes smaller. Considering that there is a trend toward increasing the plasma power in the actual manufacturing of Si devices, it is likely that the above tendencies support the superiority of use of the Y_2O_3 coatings. Within the Y_2O_3 coatings, use of larger primary particle (Y3) is effective in forming a highly durable coating at low plasma power. The influence of the primary particle size on the durability at high power, however, is found to be small.

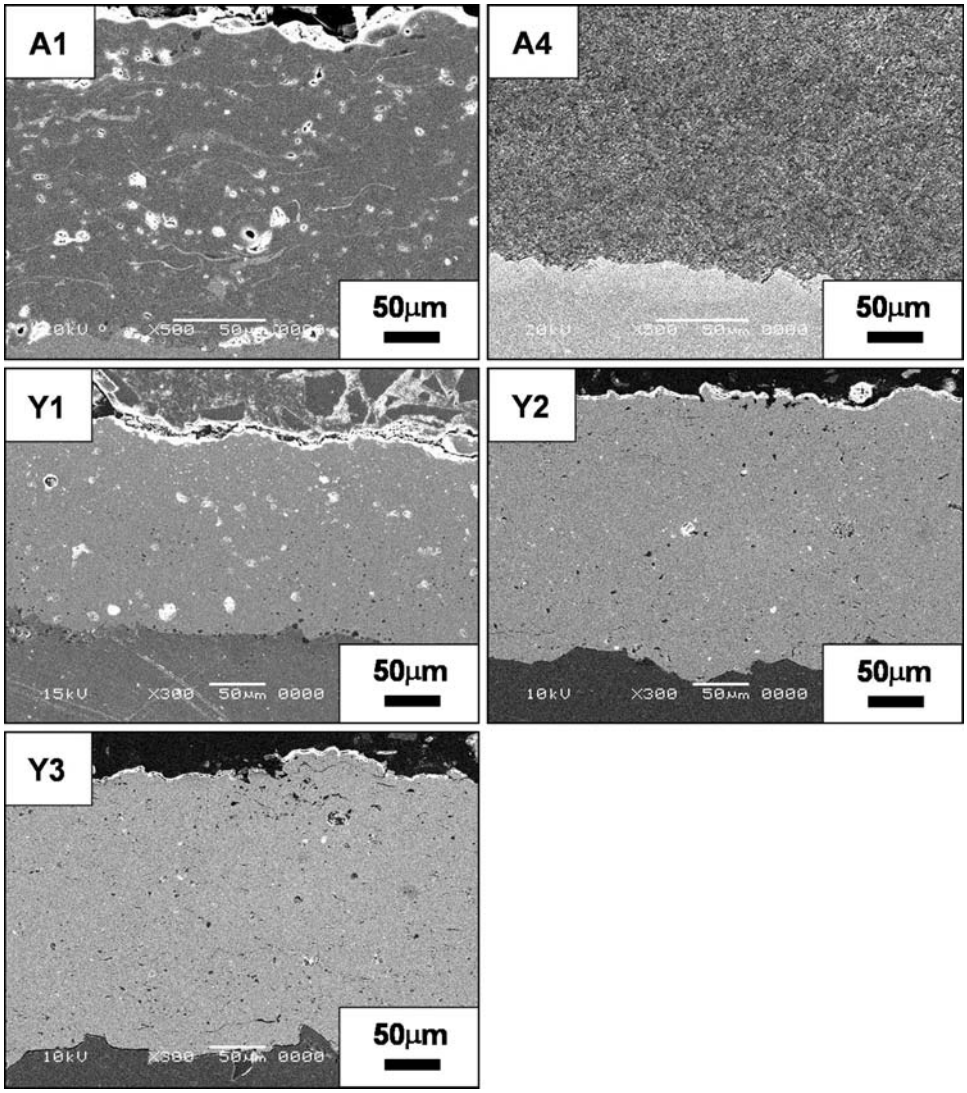

Fig. 3 Cross-sectional SEM images of as-sprayed coatings

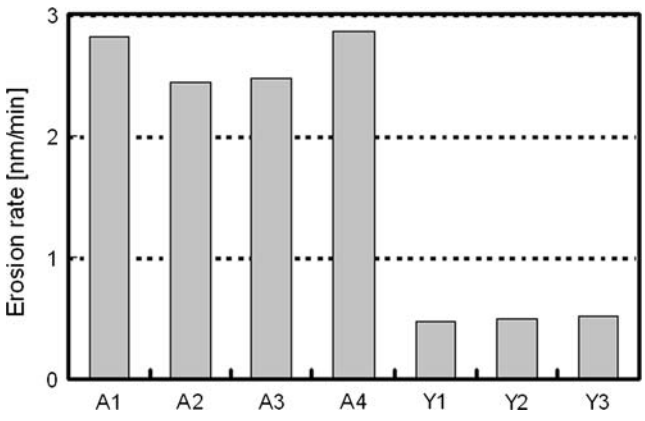

Fig. 4 Erosion rate of the spray coatings against CF_4/O_2 plasma at the low power of 80 W

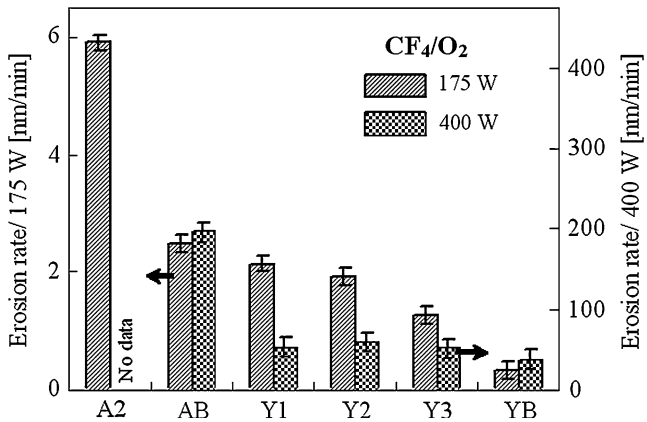

Fig. 5 Erosion rates of the plasma sprayed coatings and the sintered-bulk ceramics by CF_4/O_2 plasma at both medium (175 W) and high (400 W) power conditions

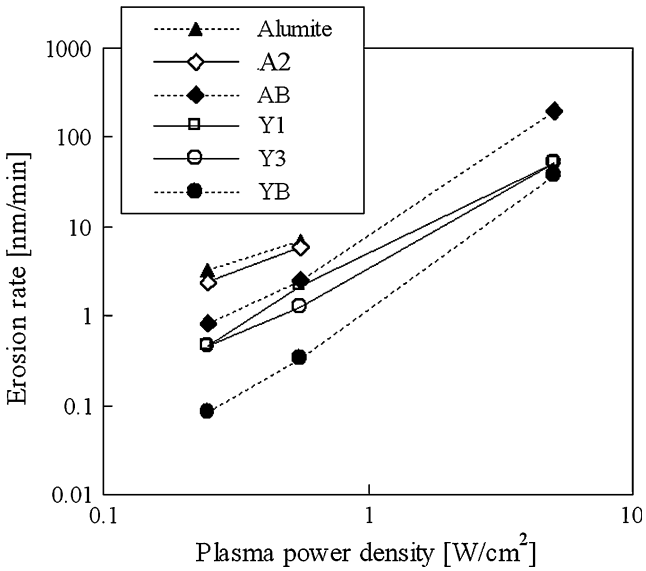

Fig. 6 Erosion rates of the spray coatings, sintered-bulk ceramics, and alumite film as a function of plasma power density

Figure 6 shows the logarithmic scaled erosion rates of the spray coatings, the sintered bulk, and conventional alumite film as a function of plasma power from 80 to 400 W, where horizontal axis is normalized as the plasma power density because effective exposure area is different from low, medium, and high power conditions. As for sintered-bulk, Y_2O_3 and Al_2O_3 have a similar tendency (similar slope), with the erosion rates being almost proportional to the square of plasma power density. The similar tendency is considered to be derived from the intrinsic properties of the ceramic materials. In the Y_2O_3 coatings, the increasing rate of the erosion rates as a function of plasma power density is lower than that of bulk ceramics. As a result, although the durability of Y_2O_3 coatings is still inferior to Y_2O_3 bulk at high power density, its difference becomes smaller with increasing power density.

3.4 Influence of Plasma Gases (CF_4/O_2 and $Ar/CF_4/O_2$)

Influence of plasma gas compositions between CF_4/O_2 and $Ar/CF_4/O_2$ is shown in Fig. 7. Little effect of primary particle size is seen at both gas conditions in the Y_2O_3 coatings (Y1-Y3). On the other hand, the influence of plasma gas composition on the erosion rates of Al_2O_3 and Y_2O_3 is clearly observed. In all Y_2O_3 specimens of the coatings and bulk, the erosion rate becomes higher at $Ar/CF_4/O_2$ plasma condition. In contrast, higher erosion rate is observed at CF_4/O_2 plasma condition in Al_2O_3 case. The difference in the influence of the gases is considered to be caused by both erosion processes by the plasma and properties of Al_2O_3 and Y_2O_3.

Coburn et al. (Ref 13) reported that the RIE etching process is an ion-assisted plasma etching process by combination of chemical etching by radicals and physical etching by ion sputtering. It is known that the etching rate

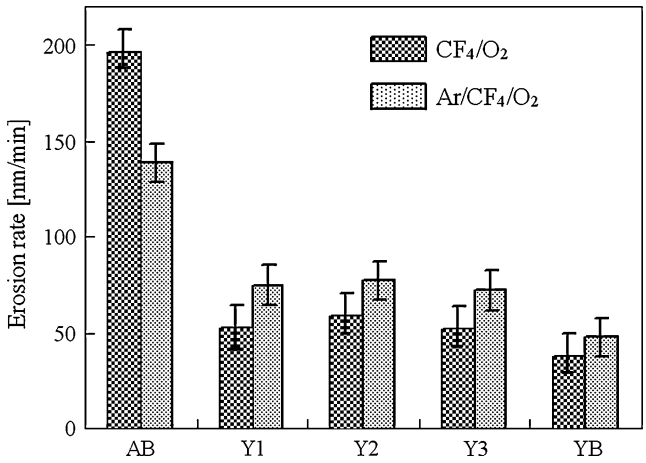

Fig. 7 Erosion rates of the spray coatings and sintered-bulk ceramics against CF_4/O_2 and $Ar/CF_4/O_2$ plasma gases at higher plasma power (400 W)

Table 6 Properties of alumina and yttria

	Standard free energy of formation ΔG (kJ/mol @373 K)	Vapor pressure (atm @1273 K)	Sputtering yield (Ar^+, 500 eV)
Al_2O_3	−1038	2×10^{-17} (AlF_3: 7×10^{-3})	1.05
Y_2O_3	−1791	5×10^{-19} (YF_3: 4×10^{-8})	0.68

increases 10 times or more with the combination compared to only physical or chemical etching in the case of Si wafer. As for gases, it is well known that CF_4 affects both chemical and physical etching. O_2 is mainly used to remove the carbon from the Si wafer by forming CO or CO_2 gases, where carbon is generated by decomposition of CF_4. Ar only affects physical etching because of its chemical stability. Properties of the Al_2O_3 and Y_2O_3, which will be related to the chemical and physical etching phenomenon, are summarized in Table 6. From the properties, it is observed that Y_2O_3 is chemically stable with a higher standard free energy of formation (ΔG), lower vapor pressure, and physically stable, low ion sputtering yield, compared to Al_2O_3, which is consistent with the results obtained in this study.

Therefore, it is suggested that difference in both ΔG and vapor pressure strongly affects in the CF_4/O_2 plasma. Yttrium has much lower vapor pressure than aluminum, about $1/10^2$ times for oxides and $1/10^5$ times for fluorides. This large difference may contribute to the large difference of the erosion rate between yttria and alumina. In the $Ar/CF_4/O_2$ plasma, on the other hand, ion sputtering effect is suggested to be stronger. Since durability of Y_2O_3 against ion sputtering is less than 2 times that of Al_2O_3, the difference of the erosion rate may be smaller.

3.5 Analysis of Eroded Surfaces by CF_4/O_2 and $Ar/CF_4/O_2$ Plasma

SEM images of the surface of the specimens after the plasma erosion test (400 W) are shown in Fig. 8.

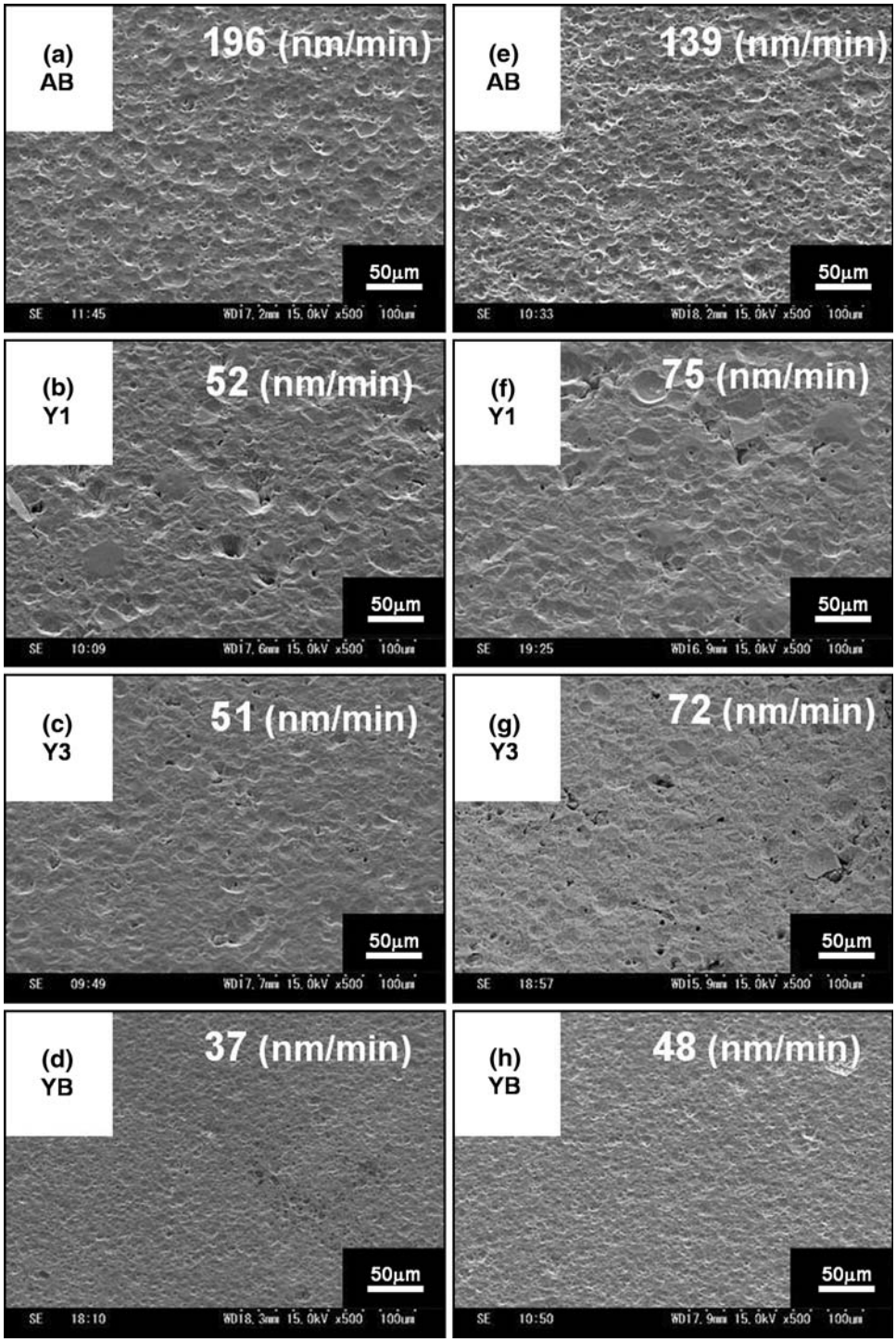

Fig. 8 SEM images of the eroded surface of the specimens: (a-d) CF_4/O_2 and (e-h) $Ar/CF_4/O_2$ showing the erosion rates

Crater-shaped pits are observed on the sintered-bulk specimens and pit size is smaller for Y_2O_3 than Al_2O_3. Within spray coatings, although the erosion rates are almost same at both conditions, surface morphologies are different, where eroded surface seems to become smoother from Y1 to Y3. Relation between roughness of the eroded surface measured by stylus method and plasma erosion rate is investigated as shown in Fig. 9. It is clear that average surface roughness (R_a) of bulk materials is lower than that of the coatings. In spite of high erosion rate for bulk Al_2O_3, the R_a is almost comparable to Y3 coating, which is smoother than Y1 coating.

It can be assumed that maintaining a smooth surface during plasma erosion prevents generating large-sized

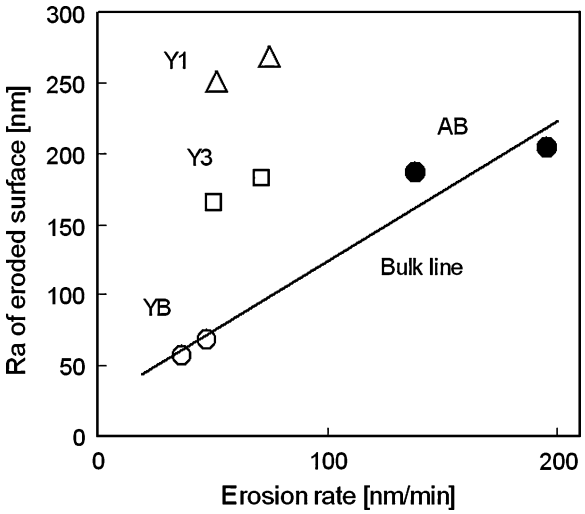

Fig. 9 Relation between average roughness (R_a) of the eroded surface measured by stylus method and plasma erosion rate

particle. As the RIE keeps evacuating using vacuum pump at etching process, small particles are easily exhausted from the chamber, which avoids deposition onto the device. Therefore, it is considered that Y3 is the most suitable coating in terms of both lower erosion rate and retaining smoother surface within the spray coatings in this study. However, Y3 coating has still higher roughness of about 3 times and higher erosion rate of about 1.5 times compared to bulk Y_2O_3. Increase of bonding strength between lamellae as well as decreasing pores should still be necessary by optimization of powder and spray parameters for improvement.

3.6 Electric Strength of the Coatings

Electric strength of the spray coatings is shown in Fig. 10, measured by typical withstand voltage tester as illustrated in Fig. 2, where the coating thickness is adjusted ranging from 200 to 300 μm. A4 coating shows the highest electric strength of about 20 kV/mm. Within plasma sprayed Al_2O_3 coatings, use of smaller powders (A2 and A3) is effective to increase the strength and a possible reason for this is the increasing density (decreasing porosity). On the other hand, purity is less affected than porosity, suggested from the result of A2 and A3 coatings. Furthermore, in spite of low purity due to both low purity powder (99.6%) and inclusion of carbon from HVOF flame, A4 coating has the highest electric strength. This could be attained from high coating density as shown in Fig. 2.

It should be noted that the use of Y_2O_3 coating for ESC is difficult without solving the problem of mechanical strength, for example, low Vicker's hardness of about 3-400HV. However, electric strength of the Y_2O_3 coatings (Y2 and Y3) is slightly higher (about 1 kV/mm) than that of A2 and A3 coatings. Considering the energy gap, which is one of the factors to define insulating properties, Y_2O_3 and Al_2O_3 have almost same value of about 6 eV (Ref 14, 15), which suggests comparable electric strength. Thus, the slight difference in electric strength may be due to the

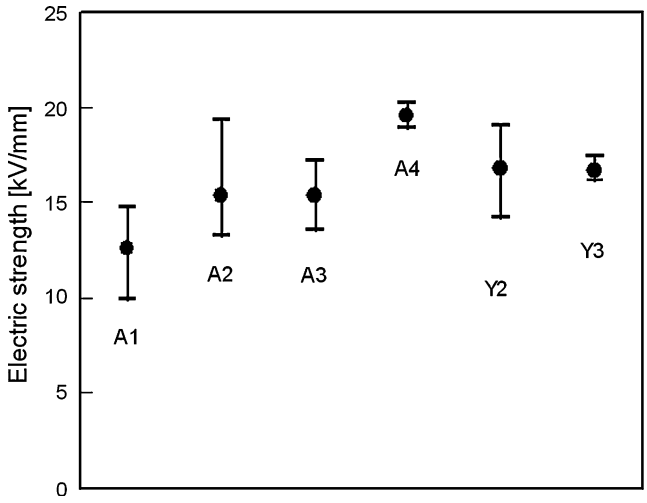

Fig. 10 Electric strength of the spray coatings

difference in coating density, which is higher for Y_2O_3 coatings as shown in Fig. 3.

Low fluctuation of the electric strength for Y3 coating suggests higher uniformity compared to Y2 coating in spite of no observation of clear difference between SEM images. This high uniformity may also result in preservation of smoother surface after the plasma erosion. It can be considered that Y3 powder produces denser coating because of low density of the agglomerated-and-sintered powder, in other word, porous powder structure as shown in Fig. 1. The porous structured powder of Y3 will easily melt during plasma flame and followed decrease of inclusion of no melting particle that degrades coating uniformity.

4. Conclusions

Structural properties of Al_2O_3 and Y_2O_3 coatings have been investigated in this study to understand the mechanism that degrades the plasma erosion resistance and electric strength. The study has arrived at the following conclusions for improving plasma erosion resistance and electric strength, which are major required properties for chamber shield and electrostatic chuck, respectively, in semiconductor and flat-panel-display production equipment.

1. Use of agglomerated-and-sintered Y_2O_3 powder consisting of larger primary particles (Y3) is effective for producing high anti-plasma erosion resistance retaining smooth surface, which may prevent generation of large-sized particles.
2. Y3 coating also shows higher electric resistance with its lower fluctuation, which suggests high uniformity in terms of low porosity as well as crystallinity.
3. Coating density strongly affects electric strength for both Al_2O_3 and Y_2O_3 coatings and the influence of purity is found to be much lower in the study. As a result, densest Al_2O_3 coating of A4 by HVOF shows best electric strength in spite of high impurity.

References

1. *Status and Perspective of Thermal Spray Markets 2004*, Digital Research Institute Inc., Nagoya, Japan, 2004, p 20-33 (in Japanese)
2. Y. Kobayashi, Current Status and Needs in the Future of Ceramics Used for Semiconductor Production Equipment, *Proc. 37th Seminar on High-Temperature Ceramics* (Osaka, Japan), Japan Ceramics Society, 2005, p 1-7 (in Japanese)
3. R. Ohtsuki, Publication of Japanese Patent Application, 2001-226773
4. J. Kitamura, H. Mizuno, N. Kato, and I. Aoki, Ceramic Coatings Prepared by Plasma Spraying for Semiconductor Production Equipments, *Mater. Trans.*, 2006, **47**(7), p 1677-1683
5. J. Kitamura, H. Mizuno, H. Ibe, and I. Aoki, Erosion Properties of Plasma Sprayed Ceramic Coatings Against Process Plasma in Semiconductor Production Equipment, *Proc. International Thermal Spray Conference 2007* (Beijing, China), ASM International, 2007, p 943-947
6. T. Morishita, S. Osawa, and T. Itsukaichi, HVOF Ceramic Coatings, *Proc. International Thermal Spray Conference 2004* (Osaka, Japan), DVS, 2004 (CD-ROM)
7. R. Westergård, L.C. Erickson, N. Axén, H.M. Hawthorne, and S. Hogmak, The Erosion and Abrasion Characteristics of Alumina Coatings Plasma Sprayed Under Different Spraying Conditions, *Tribol. Int.*, 1998, **31**(5), p 271-279
8. Y. Xie and H.M. Hawthorne, Wear Mechanism of Plasma-Sprayed Alumina Coating in Sliding Contacts with Harder Asperities, *Wear*, 1999, **225-229**, p 90-103
9. D.I. Pantelis, P. Psyllaki, and N. Alexopoulos, Tribological Behaviour of Plasma-Sprayed Al_2O_3 Coatings Under Severe Wear Conditions, *Wear*, 2000, **237**, p 197-204
10. R. Westergård, N. Axén, U. Wiklund, and S. Hogmak, An Evaluation of Plasma Sprayed Ceramic Coatings by Erosion, Abrasion and Bend Testing, *Wear*, 2000, **246**, p 12-19
11. J.R. Mawdsley, Y.J. Su, K.T. Faber, and T.F. Bernecki, Optimization of Small-Particle Plasma-Sprayed Alumina Coatings Using Designed Experiments, *Mater. Sci. Eng. A*, 2001, **308**, p 189-199
12. P.P. Psyllaki, M. Jeandin, and D.I. Pantelis, Microstructure and Wear Mechanisms of Thermal-Sprayed Alumina Coatings, *Mater. Lett.*, 2001, **47**(1-2), p 77-82
13. J.W. Coburn and H.F. Winters, Plasma Etching—A Discussion of Mechanisms, *J. Vac. Sci. Technol.*, 1979, **16**(2), p 391-403
14. I.P. Batra, Electronic Structure of α-Al_2O_3, *J. Phys. C: Solid State Phys.*, 1982, **15**, p 5399-5410
15. A. Ohta, M. Yamaoka, and S. Miyazaki, Photoelectron Spectroscopy of Ultrathin Yttrium Oxide Films on Si(100), *Microelectron. Eng.*, 2004, **72**(1-4), p 154-159